Presented at the 54th Annual Fall
Technical Conference and Exhibition
of the Society of Petroleum Engineers,
AIME, Las Vegas, NV, September 23-26, 1979

LBL-9769

CONF-790913--9

A STUDY OF THERMAL EFFECTS IN WELL TEST ANALYSIS

Donald C. Mangold, Chin Fu Tsang,
Marcelo J. Lippmann and Paul A. Witherspoon

September 1979

Prepared for the U. S. Department of Energy
under Contract W-7405-ENG-48

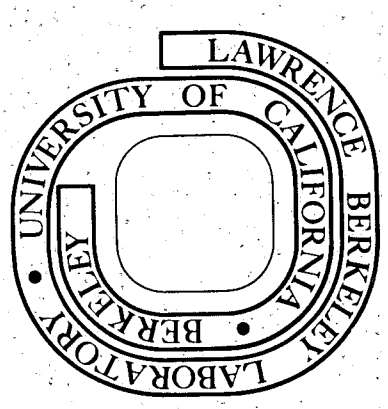

DISCLAIMER

SPE
Society of Petroleum Engineers of AIME

SPE 8232

A STUDY OF THERMAL EFFECTS IN WELL TEST ANALYSIS

by Donald C. Mangold, Chin Fu Tsang, Marcelo J. Lippmann and Paul A. Witherspoon (Member SPE-AIME), Lawrence Berkeley Laboratory, University of California, Berkeley, California

This paper was presented at the 54th Annual Fall Technical Conference and Exhibition of the Society of Petroleum Engineers of AIME, held in Las Vegas, Nevada, September 23-26, 1979.

ABSTRACT

Data analysis of well tests performed in non-isothermal (e.g., geothermal) reservoirs should take into account pressure changes resulting from fluid (and rock) temperature-dependent properties. For example the presence of zones of different temperatures may resemble permeability boundaries and will require careful interpretation of well test data. The present investigation employed a numerical model which incorporates temperature effects on fluid viscosity, density, and heat capacity. This study not only examines the influence of the viscosity variation but also the effects of the transition zone between hot and cold waters.

A series of studies were performed to simulate the results from testing a well in a hot zone which is surrounded by a concentric cooler region. Observations were made at both the well itself and at observation wells. The cases include: (1) production tests to analyze long-term transient effects; (2) build-up tests to examine pressure variations after short periods of production; (3) injection tests of colder water into the hot zone to evaluate viscosity effects; and (4) partial penetration of the aquifer to study thermal effects on tests carried out using a partially penetrating production well.

A. INTRODUCTION

A challenge to the interpretation of well test results from nonisothermal reservoirs is the effect on the pressure response due to fluid and rock temperature-dependent properties. Zones of different temperatures in the reservoir may resemble permeability boundaries, so that care in intepretation of results is required[1]. This study is an examination of these temperature effects on well test data where the producing well is completed in the center of a hot zone surrounded by a concentric cooler water region. The investigation was carried out with a view toward comparing the results of such tests with the classical Theis solution, and discovering the ways in which temperature differences can be accounted for in welltest data analysis.

References and illustrations at end of paper

Only recently have there been discussions of non-isothermal well-testing in the literature. An analytical study by Tsang and Tsang[2] motivated the present study by giving semilog results to be expected from cold water injection into a hot reservoir. By assuming a specific form for the variation of the mobility (k/μ) across the transition zone (from cold to hot water), they were able to derive solutions which follow the classic Theis curve for each region. From early and later time data reservoir transmissivity (kh/μ) and storativity (ϕch) can be determined so that compressibility (c), reservoir permeability (k), porosity (ϕ) and thickness (h) can be evaluated. Their results prompted the present numerical investigation of viscosity effects where production, build-up and partial penetration well tests are considered.

B. BACKGROUND

The standard methods of well-testing data analysis in isothermal reservoirs have been thoroughly documented by Earlougher[3]. The problems of well-testing in geothermal reservoirs have been discussed by only a few authors in the past decade. Recently Narasimhan and Witherspoon[4] have reviewed the problems in carrying out and analyzing well tests in these systems. They mention that the conventional concept of transmissivity should be replaced by absolute permeability (k) or the product kh. In another recent study[5] of reinjection at the East Mesa geothermal area, pressure distributions based on viscosity ratios of 1:1.9 between hot and cold water were described. The semilog plots show a distinctive change in slope at the cold front. The approach used, however, was a series of steady state runs with the cold front at varying distances from the production well, and with energy and mass transport equations decoupled. A paper by Rice[6] used computer models to describe drawdown and build-up tests in single phase and two-phase reservoirs under isothermal conditions. Earlier, Chappelear and Volek[7] modeled the injection of a hot liquid into a porous medium using temperature-dependent viscosity. They assumed specific heat and density were independent of temperature, and they calculated temperature (not pressure) distributions within the reservoir, caprock and bedrock. Their results show that the high viscosity of the colder water effectively controls the average

temperature and the temperature distribution within the system.

For composite reservoirs, Bixel, Larkin and Van Poollen[8] gave results for the pressure response in isothermal reservoirs with linear discontinuities, for both drawdown and build-up tests. Later, Ramey[9] made an analytical study of a well test performed in cylindrical composite reservoirs showing permeability contrasts. Even though the systems analyzed were isothermal, their behavior may be similar to nonisothermal ones. These works suggest lines for future extensions to the present study.

C. COMPUTATIONAL APPROACH

This study employed a numerical model[10] developed at Lawrence Berkeley Laboratory (LBL) called "CCC" (for Conduction-Convection-Consolidation) to simulate a geothermal reservoir with a central hot cylindrical region surrounded by colder water. The program has coupled energy and mass transport equations to simulate single phase nonisothermal saturated porous systems. Viscosity, specific heat and density of water are properly taken as temperature-dependent properties (see Tables 1 and 2). The program also has the ability to consider pressure and temperature-dependent rock and fluid properties in general, but for this study only water properties were allowed to vary with temperature. In particular, intrinsic permeability was held constant throughout in order to study variability due to viscosity alone. Pure liquid water was assumed; the effects of a salt solution of a 3wt% brine in our present problem are negligible (see Section I below). This model has been validated against a variety of analytical and semianalytical solutions, as well as field data[11-13].

The mesh design used for the majority of cases studied in this paper employs cylindrical symmetry with nodes at 1 m intervals to a distance of 300 m. This fine mesh is necessary to simulate the temperature front movements properly. The nodal separation gradually increases after 300 m up to a constant pressure and temperature boundary node at 5150 m from the well. The caprock and bedrock are assumed to be insulated and impermeable for the purposes of this study. Two sizes of the "hotspot" were investigated: a 100 m-radius case is discussed first, then a 50 m-radius hotspot is analyzed in more detail. For simplicity, in most cases a single layer model is assumed (i.e., effectively gravity is neglected). The effects of gravity and buoyancy of the hot water are considered in the case of partial penetration with a multiple layer mesh design. All cases begin with a sharp front between the hot and cold water, but the effects of a diffuse front are also commented on for several of the cases studied.

All tests are assumed to have constant mass flow rates; for the 250 °C hotspots the volumetric flow rate was set at $q = 6.0602 \times 10^{-2}$ m^3/s. There is no flashing occurring in the reservoirs. Also, wellbore effects such as the skin effect and wellbore storage are assumed negligible, since in this study the wellbore is not modeled. These assumptions are necessary in order to concentrate attention on the variations in reservoir fluid pressure and fluid temperature during the test.

D. STUDY OF THERMAL EFFECTS IN WELL TEST ANALYSIS: 100 M CASE

In this case the temperature within the cylindrical geothermal anomaly is 250 °C; the remainder of the simulated region, including the boundary node, is at 100 °C. When the usual semilog plot of ΔP versus log time is made, the slope m of the straight line will reflect the influence of the temperature on the water viscosity, μ, and the volumetric flow rate, q (due to changes in water density):

$$m = 0.183234 \frac{qB\mu}{kh}$$

For early times, the slope should reflect the values of μ and q for 250 °C. However, after the influence of 100 °C region is felt, the slope will change. Since the viscosity ratio of the water at these two temperatures is 1:2.6, and the fluid density ratio is 1:0.83, the combined effect from the different temperatures on the semilog slope is approximately 1:2. This is the change in slope m which would be expected in the presence of permeability barrier (external region half as permeable as the zone around the well), if the common assumption of an isothermal reservoir is made. Figure 1 shows the results from 39 days of production from the 100 m-radius hotspot, and for the later times the semilog slope is evidently about twice that of the initial slope.

Of course, the later slope must be exactly two times the early slope to indicate a perfect barrier. However, a slope of nearly 2 might be grounds to interpret the presence of an imperfect permeability barrier in the reservoir. Such a thermal effect could therefore cause a mistaken interpetation in the well test analysis.

The underlying pressure distribution for this case is seen in Figure 2, where the effect of the different temperature waters is evident. Even after a month of production the boundary of the colder water still provides a significant change in the pressure decline curves. Furthermore, the thermal front has barely moved during these 39 days (Figure 3). In practice, the "moving boundary" of the thermal front would probably appear to be stationary during a well test, because the radius of an actual hotspot would likely be greater than 100 m, and the mass of fluid withdrawn would only slightly affect the position of the front. Thus, the thermal boundary would not be detectable as a moving boundary, making interpretation of this change in semilog slope even more difficult to distinguish from a permeability barrier.

Finally, this effect may appear for any combination of different water temperatures. If the temperature of the surrounding region is increased from 100 °C to 175 °C, the same type of result is observed (Figure 4). Here the ratio of the semilog slopes is only 1:1.3, but a definite change in slope is nevertheless visible.

The 100 m-radius hotspot was chosen to illustrate the general case of a thermal boundary which does not move appreciably in time. Therefore, the effect of a significant fluid viscosity difference appears in the data as a stationary permeability barrier throughout nearly six weeks of production.

E. THE 50 M HOTSPOT: PRODUCTION FOR 120 DAYS

For the remainder of this study a 50 m-radius hotspot was assumed, in order to investigate effects when the production period is long enough to manifest the moving boundary of the thermal front. In this case, production was continued for 120 days, that is, until all the 250 °C water was extracted from the reservoir, which then was at 100 °C throughout. The progression in pressure change from the initial hotspot condition to the end is shown in the semilog plot of Figure 5, where there are several discernible periods of different response. During the earliest times (up to nearly 0.5 day) the pressure follows the 250 °C Theis behavior, as expected. There follows a transition time (from 0.5 to 2 days) where the curve shifts to run parallel to the 100 °C Theis curve, but still below it in magnitude (from 2 to 20 days). Then the curve again shifts upward (20 to 60 days) until the temperature front begins to reach the observation well. At this point, the pressure changes drastically, sloping steeply upward to join the 100 °C Theis curve (for times greater than 60 days), as it should since by the end of the 120 days the entire reservoir is at 100 °C.

Two observations can be made on the basis of such a complete pressure history. First, as noted in the previous section, the initial period of 250 °C Theis curve behavior is followed by a transition to a curve parallel to the colder water Theis solution. Secondly, as the well continues to be produced, the curve shifts upward again as an indication of another boundary, in this case the moving boundary of the thermal front.

The practical application of this "second shift" is made by locating an observation well at some distance away from the produced well. As Figure 6 shows, the effect of the moving thermal front occurs much earlier (at approximately 15 days) when observed at a distance of 19.5 m from the production well. Thus the length of time for the moving boundary to be manifested can be minimized by data taken at a suitably distant observation well.

However, if the observation well is too far away from the axis of the hotspot, it may be in the cold water zone. Figure 7 reveals that the same general shift of curves takes place, but within a much shorter length of time (approximately 7 days). This well is at 59.5 m from the producing well, or 9.5 m outside the outer boundary of the hotspot. It is interesting to note that its early time behavior nevertheless follows a 250 °C Theis curve before shifting over to the 100 °C Theis curve. Clearly, employing one or more observation wells provides a ready check on the usual semilog direct analysis from a single well, and increases the real possibility of detection of the moving thermal boundary.

As a further examination of these results, log ΔP versus log t/r^2 curves were plotted for r = 2.5 m, 19.5 m, 39.5 m, and 59.5 m (see Figure 8, where the Theis curves for 100 °C and 250 °C are shown for reference). The observations at 59.5 m and 39.5 m eventually merge into the 100 °C Theis curve. From all the t/r^2 curves we can see that the departure from the 250 °C Theis behavior occurs at smaller values of t/r^2 for greater radial distances r from the well. Also, the merging of the pressure behavior with the 100 °C Theis solution happens at earlier values of t/r^2 for greater r. This confirms the use of more than one observation well at different radial distances from the producing well to monitor a well test, in order to trace pressure behavior which may be related to a thermal boundary.

A usual type curve matching procedure was applied to the log-log plot of r = 2.5 m data in order to estimate transmissivity (kh/μ) and storativity (ϕch). The results of the type curve analysis are given in Appendix 1. The match with the very early part of the curve (part [A]) yields a good estimate for kh/μ, as expected. But under such a direct analysis, if the analyst matched the later portion of the curve, he would be seriously mistaken (part [B]). The estimated values for ϕch reflect the sensitivity of type curve matching, even for the early time data. Again, matching with the latest portion of the curve would lead to serious errors by direct analysis.

The progress of the temperature front is interesting to follow. In Figure 9 a sequence of curves shows how the front moves slowly at first, and quite rapidly at the end, reflecting differences in radial volume under a constant pumping rate. The diffusion of the front is very apparent; Table 3 gives values for the size of the front throughout its history, and a comparison with a simple analytical conduction model[14]. This diffusion of the temperature front may also account for some of the shifting of the pressure change data curves over the period of production (see Section I below).

F. THE 50 M HOTSPOT: BUILD-UP TESTS

The build-up tests performed in this series of simulations confirm the same general behavior observed in the production tests, but the effects occur at earlier times. Figure 10 shows a Horner plot of a build-up test after 30 days of production from the 50 m hotspot of the previous section. At the earliest times the points are parallel to the 250 °C analytical curve, but after less than one day the points shift toward the 100 °C curve. By 5 days the pressure is already following characteristic 100 °C build-up behavior.

The build-up test has several differences from a production well test. First, the response is generally faster than the drawdown test. Second, because there is only mass flow resulting from pressure equilibration, the thermal front moves very little during build-up. Third, the small mass flow also means that the diffusion of the thermal front proceeds much more slowly because it is mainly by conduction. These latter two conditions do not permit the observation of a moving thermal boundary or a diffuse front as a means of discovering thermal effects, such as during drawdown tests. However, build-up tests should allow a better correlation to the proper analytical solution once a thermal front is suspected. Therefore, the best approach may be a combination of drawdown and build-up tests. The production tests would provide an analyst with sufficient data to determine kh/μ, ϕch and the presence of a moving thermal front. Then the data from build-up tests could be used to confirm the estimated values of the reservoir parameters, and to match the pressure response to type curves to discover possible thermal effects.

Similar behavior on build-up tests was observed for other combinations of temperatures. In Figure 11

the fluid viscosity ratio for 125 ° to 50 °C is approximately 1:2.4, and in Figure 12 for 250 ° to 50 °C it is about 1:5.1. Although both of these cases are for production times of only 15 days, by the end of another 15 days of shutting-in the well the pressures are responding according to the analytical solution for 50 °C. This demonstrates the rapid adjustment of the system under a variety of temperatures, and confirms that build-up tests should prove to be a useful means for checking suspected thermal effects in well testing.

G. REINJECTION AND PRODUCTION OF COLD WATER

An analytical solution has been found for geothermal reservoir pressure response to cold water reinjection (see Tsang and Tsang[2]), as mentioned above. Their general solution has been obtained by assuming that the mobility $K(z) = k/\mu$ may be represented for any $z = r^2/t$ by a smooth function which takes on the values of K_I(injection), K_R(reservoir) and $(K_I + K_R)/2$, respectively, at $z = 0$, $z = \infty$, and z = mean radial distance of the (symmetric) thermal front. Their results indicate that for small values of t/r^2 the curve follows a Theis solution with parameters corresponding to those of the native hot water. For large t/r^2 it approaches a line parallel to a Theis line with parameters corresponding to those of the injected water. It is suggested that from matching early data kh and ϕch may be ascertained, and after matching later data the position of the front, and therefore h, may be estimated. Thus k, ϕc and h are evaluated. However, this procedure has not yet been tested with field data.

The results of the analytical solution were checked against the numerical model CCC employed here; one example is displayed in Figure 13. The characteristic pressure behavior noted in previous sections for drawdown and build-up tests is also apparent here, and follows the behavior predicted by the analytical solution. Later the data should begin a further shift toward the Theis solution for the injected cold water, and eventually it should merge into the pressure response for cold water alone.

To corroborate these results, the behavior of a 100 °C 50 m-radius "coldspot" surrounded by a 250 °C region was studied. It was produced for 30 days in the same fashion as the previous "hotspot" cases, with the results shown in Figure 14. Again, the pattern is the same, but now in the opposite direction (from cold water behavior toward hot water behavior). After the data runs parallel to the 250 °C Theis solution it shifts further toward that solution, but runs nearly horizontal for the last 5 days. This is probably because the 250 °C water flows much more readily than the 100 °C water, so that the produced well appears to have a full recharge boundary at this point in time. As the coldspot is produced for longer times, the data should turn further toward the 250 °C Theis solution and finally merge with it.

Thus, the effect of cold water injected or produced from hotter reservoirs conforms to the expected pattern due to fluid viscosity (and density) differences.

H. PARTIAL PENETRATION HOTSPOT

The previous sections have assumed a single layer model where there is necessarily full penetration, and gravity is not an influence. To study thermal effects in the common situation of partial penetration, a multilayered cylindrical mesh was used. There were five 10 meter thick layers in the aquifer, with nodes at radial distances of 1 m out to a distance of 20 m from the well; from 20 m outwards the size of the annular nodes gradually increased. The boundary between hot and cold regions was placed at 48 m. The well was produced for 40 days from the top two layers at 40% of the former rate. The observation well is in the middle layer, 2.5 m from the axis of the system. The results are displayed in Figure 15.

The same general pattern of the previous sections is apparent for partial penetration. The analytical solutions are taken from Witherspoon, et al.[15], and are semilog straight lines for the times plotted for the reservoir parameters used. This result confirms the effect of viscosity differences on the pressure response during a drawdown test, even when the well is partially penetrating.

I. THREE ADDITIONAL FACTORS

There are three factors which have a possible influence on the above results: the effect of natural convection, the effect of a brine solution, and the effect of a diffuse front. These possibilities are covered briefly in this section.

To study the effect of natural convection, a simulation was performed using the partial penetration mesh of 5 layers, with temperatures of 250 °C inside and 100 °C outside. There was no production at the well. After 27.5 days the mass flow cycle in the simulation achieved a quasi-steady-state and no further mass flow was computed; the heat flow calculations were continued to 38 days. The results were compared to analytical formulas recently derived by Goran Hellstrom[16] at LBL for buoyancy tilting of a thermal front in an aquifer, including the effect of a diffuse front. The numerically computed flow velocity at the front compared to within 0.76% of the analytical solution at 27.5 days. The maximum flow velocity due to natural convection was $1.455\ 10^{-7}$ m/s, compared to the flow velocity from pumping which was $4.285\ 10^{-6}$ m/s at 30 days, a factor of nearly 30:1. These results confirm that the use of a single-layer mesh for the major part of this investigation was acceptable, since natural convection has negligible effect on reservoir pressure for the time periods considered (up to approximately 40 days).

The effect of a brine solution instead of pure water was examined using estimation formulas from Wahl[17] for physical properties of geothermal brines. The results are displayed in Table 4. A 3wt% brine (30,000 ppm total dissolved solids) was chosen for comparison, because many geothermal areas (New Zealand, Japan, Mexico, U.S. [except Salton Sea], Iceland) have a smaller weight percent of total dissolved solids. The difference in properties between such a brine and water is negligible for ρC, and approximately 6% for μ or (k/μ). However, the error of 6% applies equally to the 250° and 100 °C waters, so that the viscosity ratio remains the same. Thus encountering a brine solution in place of pure water in a field test should not affect the results reported here.

Finally, the diffuseness of the thermal front will have an effect on the slope of the semilog plot, as shown in Tsang and Tsang[2]. In their analytical formulas, the size of the diffuse zone (where the viscosity varies appreciably between the values for hot and cold water) depends on the aquifer diffusivity. The smaller the value of the diffusivity, the more the semilog straight line will turn to follow the Theis curve for the injected cold water. According to their numerical results, the value used for aquifer diffusivity in this investigation would lead to a curve which turns early to run parallel to the Theis curve for colder water. Thus the present set of simulations does confirm their analytical results for the effect of the diffuse between hot and cold waters on pressure response in a well test.

J. CONCLUSION

This paper has shown that the effects of viscosity from regions of different temperature water can appear in well test data in a way that may be mistaken as permeability barriers in some cases. This effect can be recognized by a pumping test of sufficient duration with observation wells located at a suitable distance from the production well. The questions of identifying the moving thermal boundary, applications of the method to build-up tests, and partially penetrating wells have been discussed. The possible influences of gravity and buoyancy (i.e., natural convection), a brine solution, and the size of the diffuse zone have also been considered.

Future extensions of this investigation would include further work in deriving the analytical relationship between the time of departure from the Theis solution for the inner region and the distance to the boundary between the hot and cold waters, possibly along the line of Ramey[9]. With such a relationship there is the potential that geothermal well-testing could point out the presence of different temperature regions.

NOMENCLATURE

B	reservoir volumes per standard volume, dimensionless
c	fluid compressibility, Pa^{-1}
C	fluid specific heat, J/kg·K
C_a	aquifer specific heat, J/kg·K
h	aquifer thickness, m
k	intrinsic permeability, m^2
K_M	thermal conductivity of solid-fluid mixture, W/m·K
$K(z)$	mobility (k/μ), $m^2/Pa·s$
m	slope of semilog straight line, Pa/log cycle
P	fluid (pore) pressure, Pa
P_D	fluid pressure, dimensionless
q	volumetric flow rate, m^3/s
r	radial distance, m
S_s	specific storage coefficient, m^{-1}
T	temperature, °C
T_o	reference water temperature, °C
t	time, s
t_D	time, dimensionless
z	ratio r^2/t, m^2/s
α	first coefficient of thermal expansion for water, $°C^{-1}$
β	second coefficient of thermal expansion for water, $°C^{-2}$
κ	water compressibility, Pa^{-1}
μ	fluid viscosity (dynamic), Pa·s
ρ	fluid density, kg/m^3
ρ_a	aquifer rock density, kg/m^3
ρ_o	reference water density, kg/m^3
ϕ	porosity, dimensionless

SUBSCRIPTS

a	aquifer
D	dimensionless quantity
M	mixture of solid and fluid
m	match value from type curve analysis
o	reference quantity
s	specific storage
TC	Theis Curve estimate

ACKNOWLEDGEMENT

This work was supported by the U.S. Department of Energy under contract No. W-7405-ENG-48.

REFERENCES

1. Tsang, C.F., et al., "Numerical Modeling Studies in Well Test Analysis," Proceedings, 2nd Invitational Well testing Symposium, Lawrence Berkeley Laboratory LBL Report 8883, Berkeley, CA (Oct. 25-27, 1978), pp. 47-57.

2. Tsang, Y.W., and Tsang, C.F., "An Analytic Study of Geothermal Reservoir Pressure Response to Cold Water Reinjection," Proceedings, 4th Stanford Workshop on Geothermal Reservoir Engineering, Stanford, CA. (Dec. 13-15, 1978), pp. 322-331.

3. Earlougher, R.C., Jr., Advances in Well Test Analysis, SPE Monograph No. 5, Society of Petroleum Engineers of AIME, Dallas, Texas (1977).

4. Narasimhan, T.N., and Witherspoon, P.A., "Geothermal Well Testing," Lawrence Berkeley Laboratory Report 8290, Berkeley, CA (Jan. 1979).

5. Howard, J., et al., "Geothermal Resource and Reservoir Investigations of U.S. Bureau of Reclamation Leaseholds at East Mesa, Imperial Valley, California," Lawrence Berkeley Laboratory Report 7094, Berkeley, CA (Oct. 1978).

6. Rice, L.F., "Pressure Drawdown and Buildup Analyses in Geothermal Reservoirs," Proceedings, 11th Intersociety Energy Conversion Engineering Conference, vol. I, State Line, Nevada (Sept. 12-17, 1976).

7. Chappelear, J.E., and Volek, C.W., "The Injection of a Hot Liquid into a Porous Medium," SPE Journal, (March, 1969), pp. 100-114.

8. Bixel, H.C., Larkin, B.K., and Van Poollen, H.K., "Effect of Linear Discontinuities on Pressure Build-Up and Drawdown Behavior," Journal of Petroleum Technology, (Aug. 1963), 15, pp. 885-895.

9. Ramey, H.J., Jr., "Approximate Solutions for Unsteady Liquid Flow in Composite Reservoirs," Journal of Canadian Petroleum Technology, (Jan-March, 1970), pp. 32-37.

10. Lippmann, M.J., Tsang, C.F., and Witherspoon, P.A., "Analysis of the Response of Geothermal Reservoirs under Injection and Production Procedures," paper SPE-6537, presented at the 47th Annual California Regional Meeting SPE-AIME, Bakersfield, CA April 13-15, 1977.

11. Tsang, C.F., et al., "Numerical Modeling of Cyclic Storage of Hot Water in Aquifers," Lawrence Berkeley Laboratory Report 5929, Berkeley, CA (January 1977).

12. Mangold, D., Wollenberg, H., and Tsang, C.F., "Thermal Effects in Overlying Sedimentary Rock from In-Situ Combustion of a Coal Seam," Lawrence Berkeley Laboratory Report 8172, Berkeley, CA (Sept. 1978).

13. Busheck, T., Doughty, C., and Tsang, C.F., "Report on Modeling of Auburn Field Experiment," Lawrence Berkeley Laboratory Report Berkeley, CA (forthcoming).

14. Carslaw, H.S. and Jaeger, J.C., Conduction of Heat in Solids, 2nd edit., Oxford Univ. Press, Oxford, 510 p., 1959.

15. Witherspoon, P.A., et al., "Interpretation of Aquifer Gas Storage Conditions from Water Pumping Tests", American Gas Assoc., N.Y., 273 p., 1967.

16. Hellström, G., "Thermal Stratification and Buoyancy Flow," Lawrence Berkeley Laboratory Report, Berkeley, CA (forthcoming).

17. Wahl, E.F., Geothermal Energy Utilization, Wiley-Interscience, N.Y., 302 p., 1977.

APPENDIX 1

Theis Curve Matching

These calculations are for the 50 m-radius hot-spot, 250 °C inside and 100 °C outside.

A. Early Times (up to 0.372 d)

At match point, for $t_D = 10.0$ there is $\Delta P = 4.0 \times 10^5$ Pa at $t = 0.026$ d for flow rate $q = 6.0602 \times 10^{-2}$ m^3/s.

$$\left(\frac{kh}{\mu}\right)_{TC} = \frac{q}{4\pi}\left(\frac{P_D}{P}\right)_m = 1.2056 \times 10^{-8} \text{ (m}^3\text{/Pa·s)}$$

The true value is 1.3551×10^{-8}, so the analysis has a relative error of 11%.

$$\phi ch_{TC} = \left(\frac{kh}{\mu}\right)_{TC} \frac{1}{r^2}\left(\frac{t}{t_D}\right)_m = 4.3333 \times 10^{-7} \text{ (m/Pa)}$$

The true value is 2.4962×10^{-7}, so the analysis has a relative error of 74%.

B. Later Times (from 1.5 d)

At match point, for $t_D = 10.0$ there is $\Delta P = 7.3 \times 10^5$ Pa at $t = 0.53$ d (same flow rate).

$$\left(\frac{kh}{\mu}\right)_{TC} = 6.6062 \times 10^{-9} \text{ (m}^3\text{/Pa·s)}$$

The true value is 1.3551×10^{-8}, so the analysis has a relative error of 51%.

$$\phi ch_{TC} = 4.8402 \times 10^{-6} \text{ (m/Pa)}$$

The true value was 2.4962×10^{-7}, so the analysis has a relative error of 1,839%.

TABLE 1

Properties of the Aquifer Used in the Simulations

Thickness, h (m)	50
Porosity, ϕ	0.1
Intrinsic Permeability, k (10^{-3} μm^2)	29
Specific Storage Coefficient, S_s (m^{-1})	3.9×10^{-5}
Density, ρ_a (kg/m^3)	2650
Heat Capacity, C_a (J/kg·K)	970
Thermal Conductivity, K_M (W/m·K)	2.8935

TABLE 2

Properties of Water Used in the Simulations

Compressibility, κ (Pa^{-1})	6.5×10^{-10}
First Coefficient of Thermal Expansion, α (°C^{-1})	3.17×10^{-4}
Second Coefficient of Thermal Expansion, β (°C^{-2})	2.56×10^{-6}
Reference Temperature, T_o (°C)	25
Reference Density, ρ_o (kg/m^3)	996.9

Density equation:

$$\rho = \rho_o [1 - \alpha (T-T_o) - \beta (T-T_o)^2]$$

Temp. (°C)	Viscosity μ (10^{-3} Pa·s)	Heat Capacity C(J/kg·K)	Density ρ (kg/m^3)
50	0.5450	4010	987.40
100	0.2800	3770	958.84
125	0.2310	3651	939.78
175	0.1585	3434	892.08
250	0.1070	3188	796.60

TABLE 3

Diffusion of Thermal Front
120 Day Production

Time (d)	Location (m)	10% Limit (115 °C) (m)	Analytical Calc. (m)	90% Limit (235 °C) (m)	Analytical Calc. (m)	Size of Front (m)
0.15	50	—	—	—	—	0
5.00	49.5	51	—	47.5	—	3.5
20.00	45	48.5	46	40.5	44	8
35.00	40	44	42	35	38	9
59.00	30	35.5	33	24	27	11.5
77.00	20	27	24.5	9	15	18
87.00	10	21	14.5	0	5	21
91.00	Well	17.5	—	—	—	—

TABLE 4

Comparison of the Properties of Pure Water
With a 3 wt% Brine
(3 wt% = 30,000 ppm total dissolved solids)

Property	Temp. (°C)	Brine	Water	Percent Change
Density, ρ (kg/m^3)	250	818.52	796.60	2.75
	100	981.79	958.84	2.39
Heat Capacity, C (J/kg·K)	250	3092	3188	-3.00
	100	3657	3770	-3.00
Viscosity, μ (10^{-3} Pa·s)	250	0.1140	0.1070	6.54
	100	0.2983	0.2800	6.54
Density-Capacity Product, ρC (10^6 J/m^3·K)	250	2.5309	2.5396	-0.34
	100	3.5904	3.6148	-0.68
Mobility, k/μ (10^{-10} m^2/Pa·s)	250	2.5439	2.7103	-6.14
	100	.9722	1.0357	-6.14

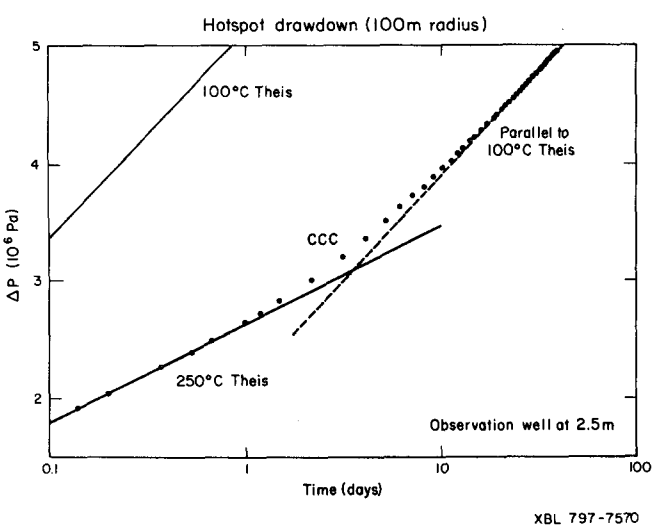

Figure 1. Drawdown curve for 100 m hotspot (r = 2.5 m).

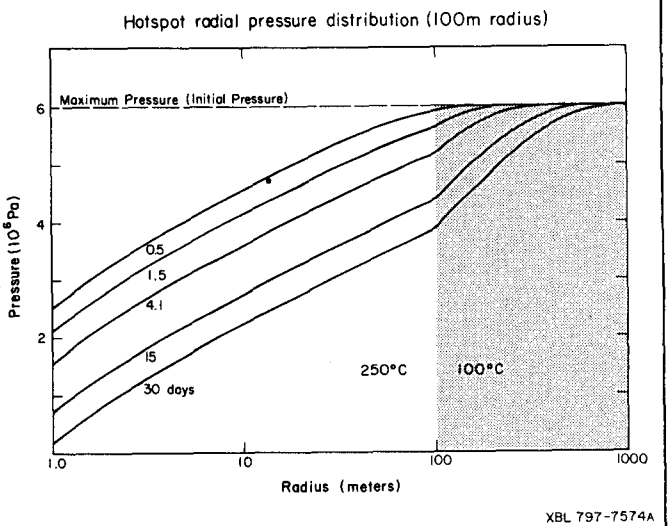

Figure 2. Radial pressure distribution for 100 m hotspot (shaded region is 100 °C).

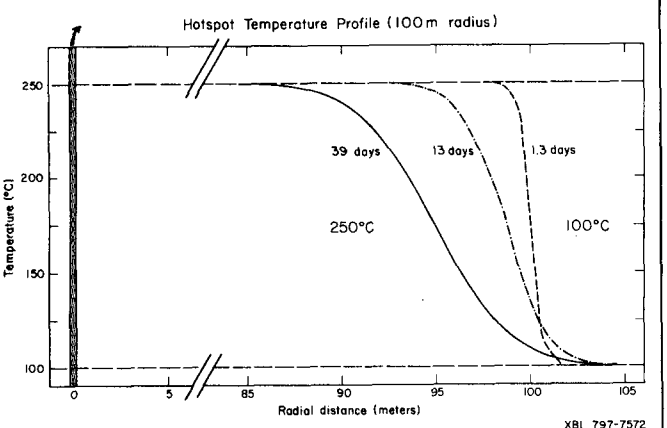

Figure 3. Temperature profile for 100 m hotspot (note break in horizontal axis).

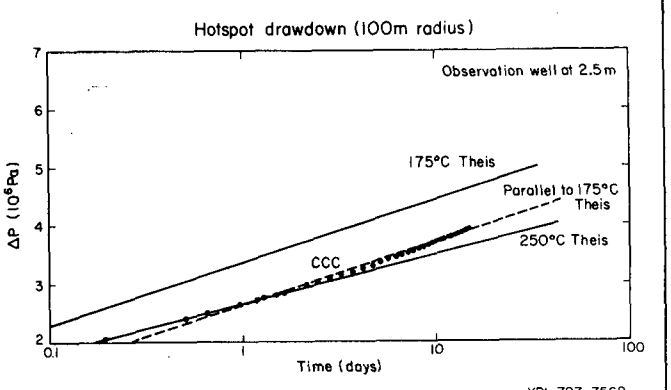

Figure 4. Drawdown curve for 100 hotspot with 175 °C for surrounding region (r = 2.5 m).

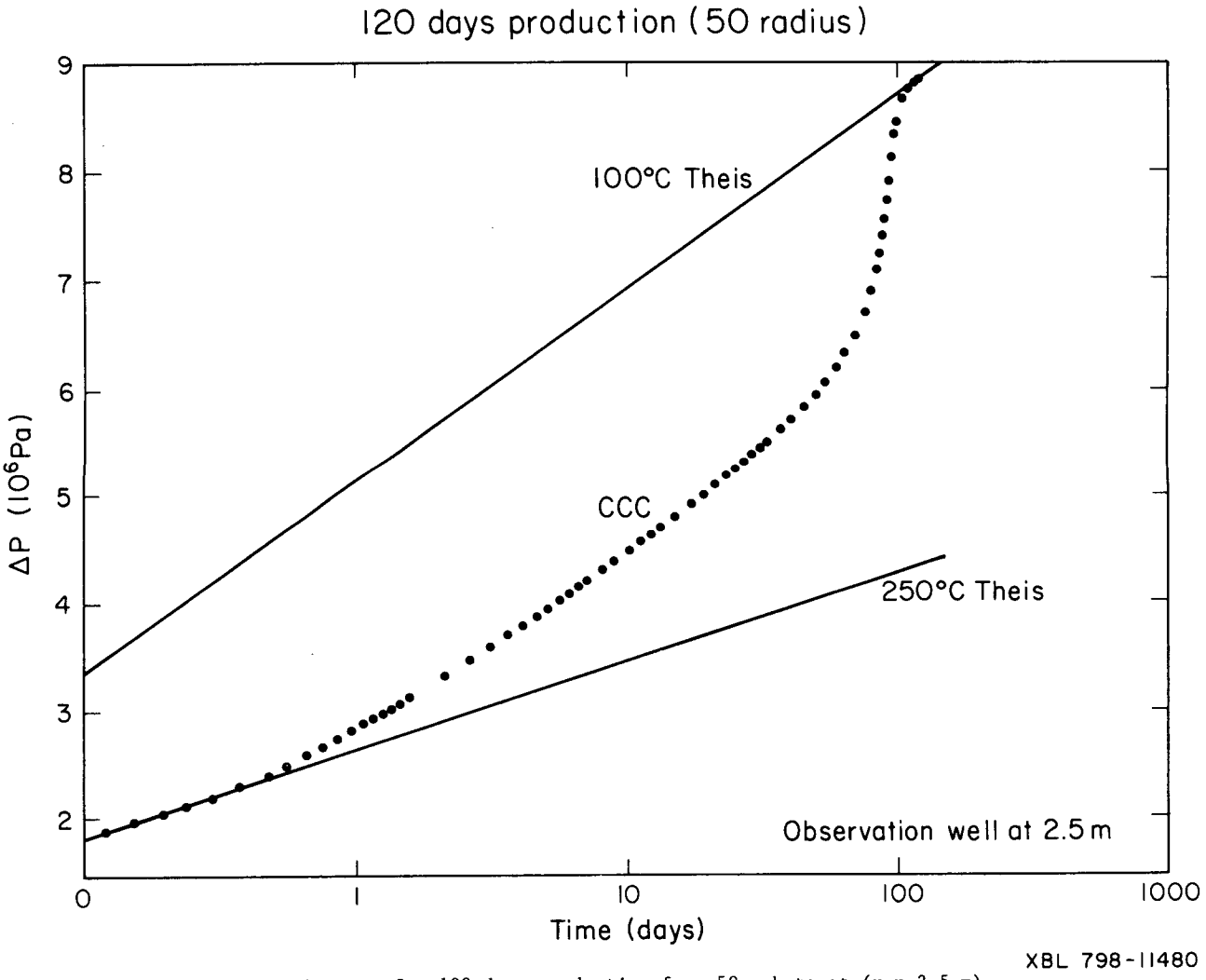

Figure 5. Drawdown history for 120 days production from 50 m hotspot (r = 2.5 m).

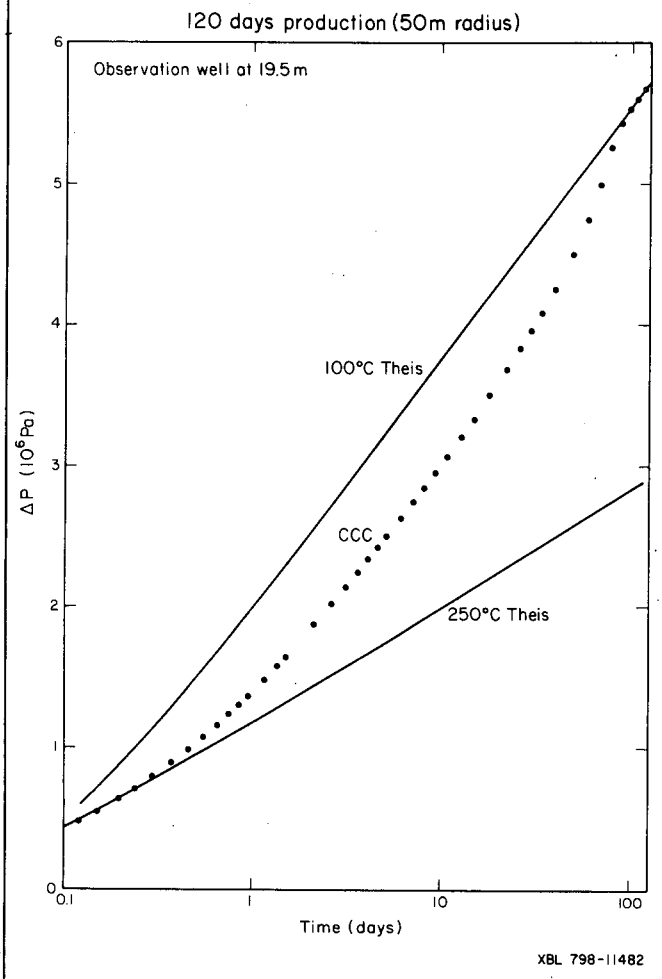

Figure 6. Drawdown history for 120 days production from 50 m hotspot (r = 19.5 m).

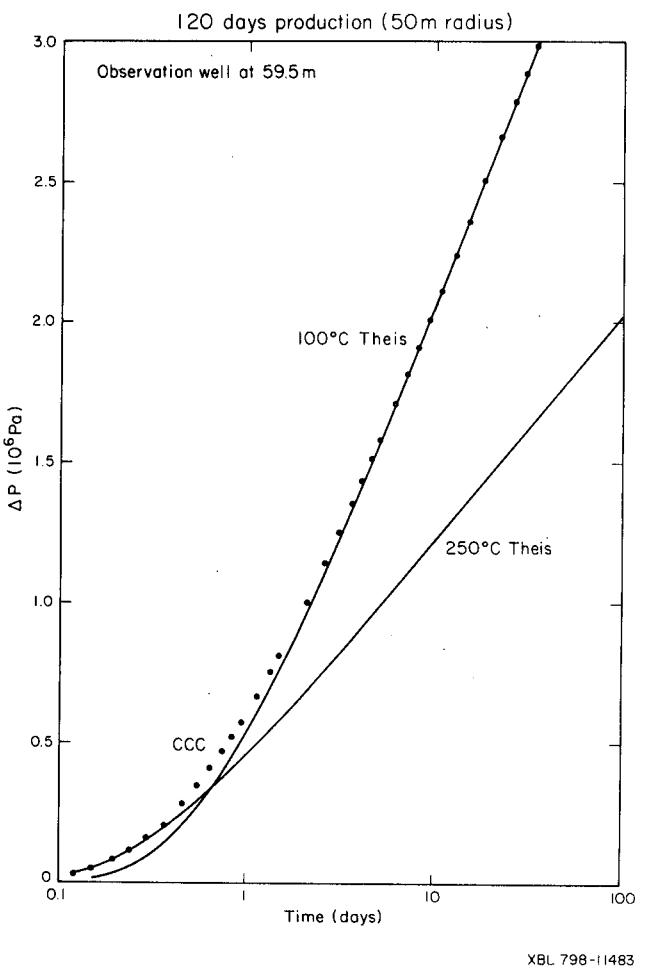

Figure 7. Drawdown history for 120 days production from 50 m hotspot (r = 59.5 m).

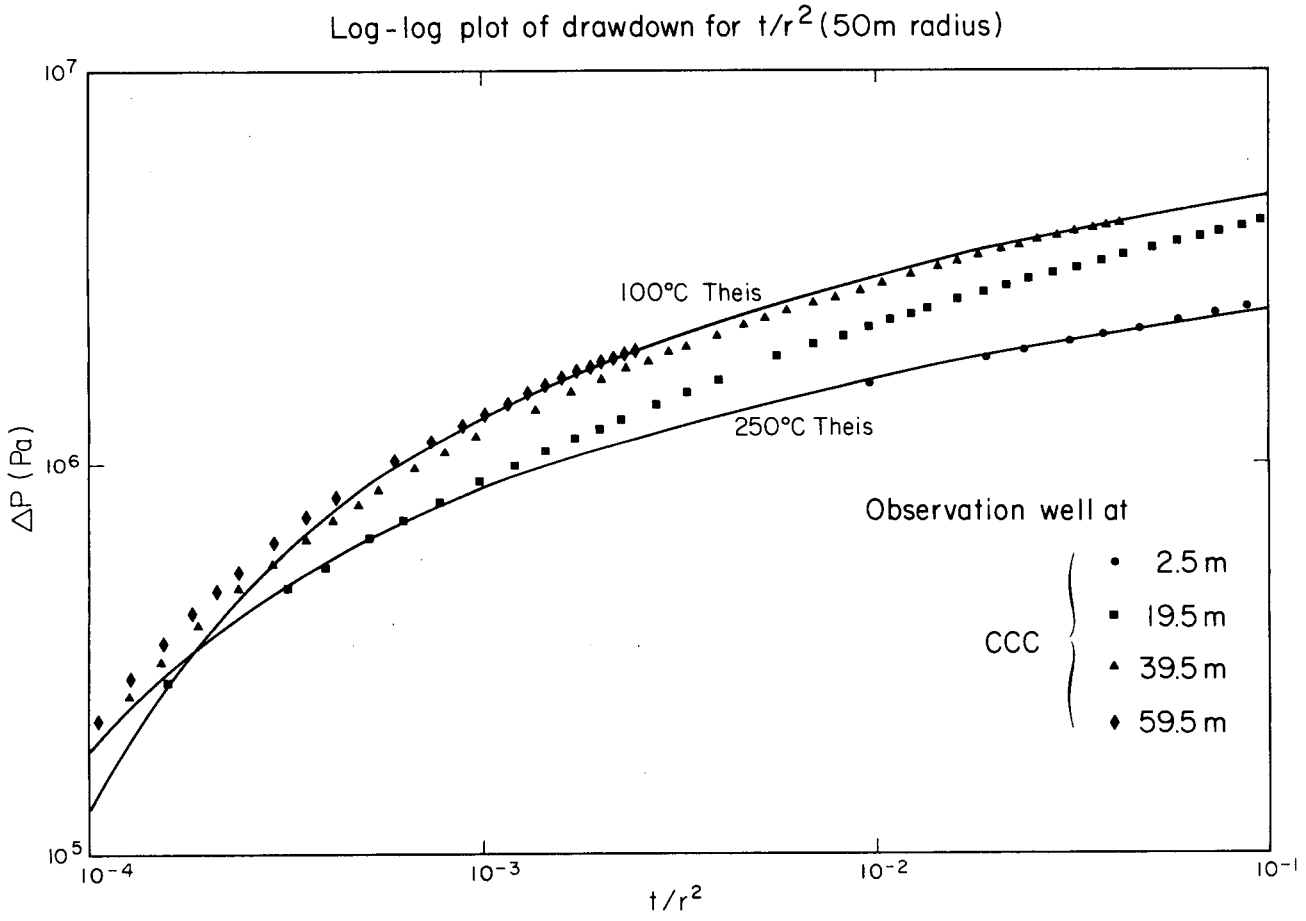

XBL 798-11496

Figure 8. Drawdown curves for t/r^2 for various radial distances r from the well (log-log plot).

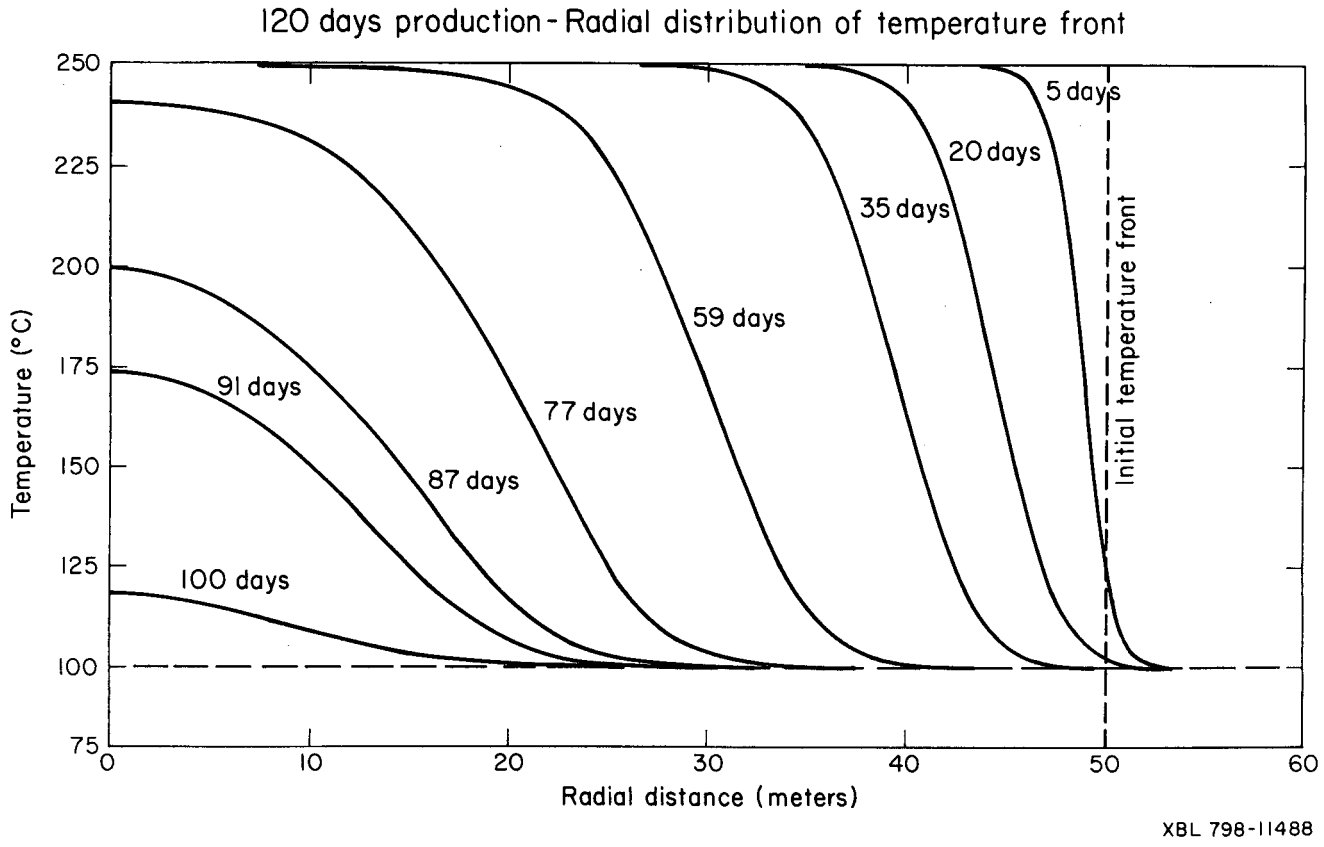

Figure 9. Radial distribution of temperature front for 120 days production from 50 m hotspot.

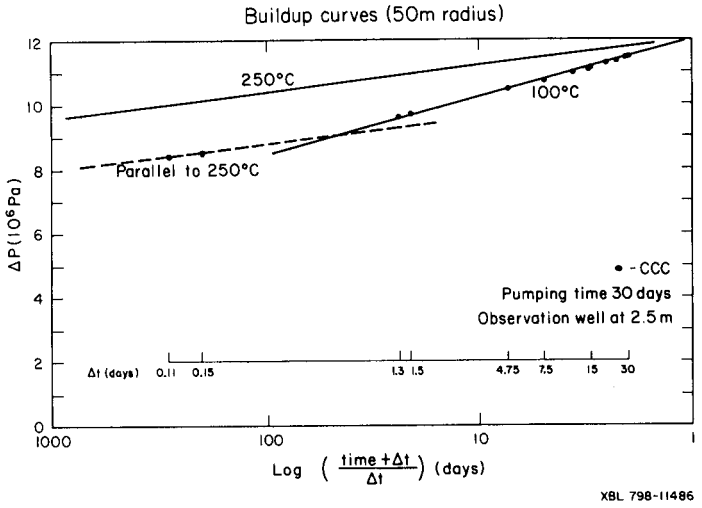

Figure 10. Buildup curves for 50 m hotspot, 250 °C and 100 °C, (after 30 days pumping, r = 2.5 m).

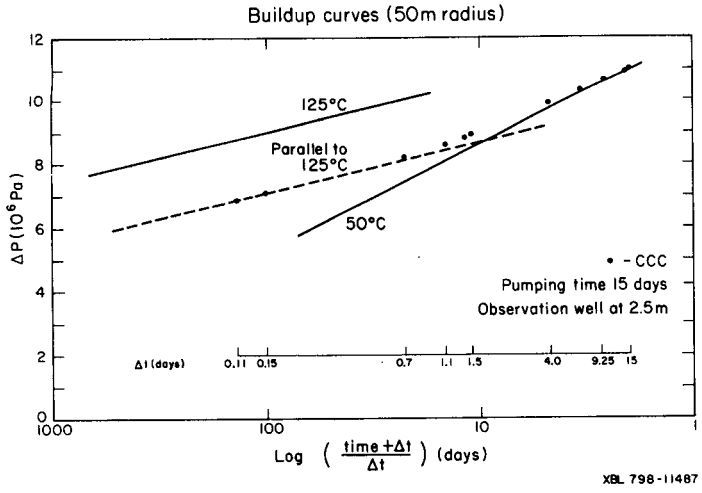

Figure 11. Buildup curves for 50 m hotspot, 125 °C and 50 °C, (after 15 days pumping, r = 2.5 m).

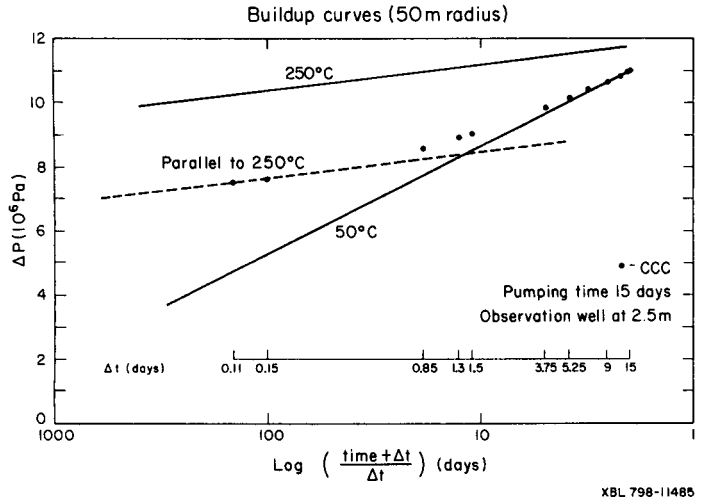

Figure 12. Buildup curves for 50 m hotspot, 250 °C and 50 °C, (after 15 days pumping, r = 2.5 m).

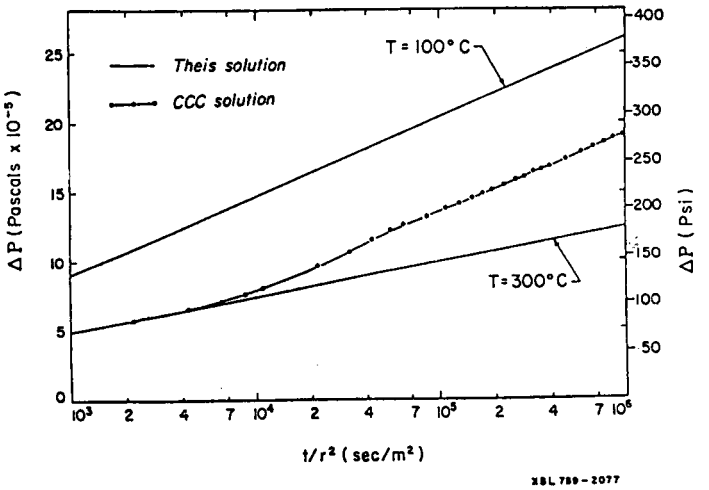

Figure 13. Drawdown curve for t/r^2 for cold water injection into a hot reservoir - see reference 2 (log-log plot).

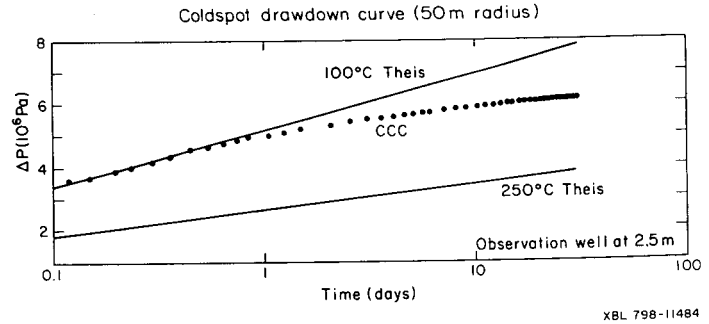

Figure 14. Drawdown curve for 50 m coldspot (r = 2.5 m).

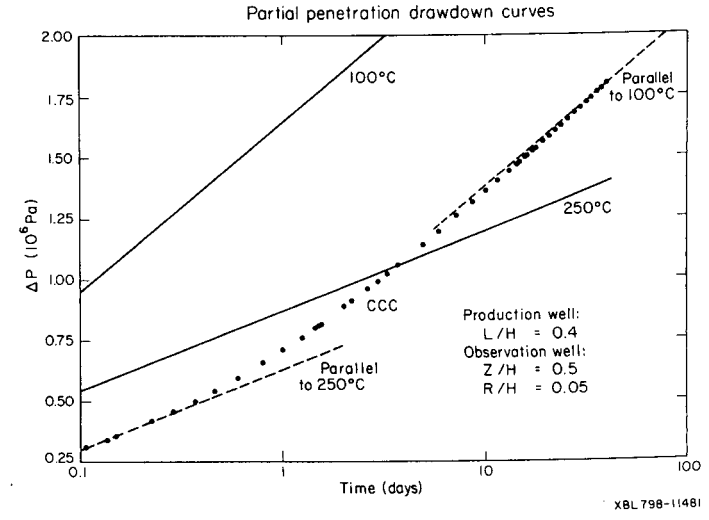

Figure 15. Drawdown curve for 40% partial penetration in 48 m hotspot.

TECHNICAL INFORMATION DEPARTMENT
LAWRENCE BERKELEY LABORATORY
UNIVERSITY OF CALIFORNIA
BERKELEY, CALIFORNIA 94720